Electronic Supplementary Material (ESI) for Materials Chemistry Frontiers.

Growth of Robust Metal-Organic Framework Films by Spontaneous Oxidation of Metal Substrate for NO_2 Sensing

Jun Zhang[ab]*, Enlai Hu[b], Fang Liu[a], Hongjun Li[b] and Tifeng Xia[a]*

[a] Institute of Materials, China Academy of Engineering Physics, Mianyang 621907, China. E-mail: j-zhang@caep.cn, xiatifeng@caep.cn.

[b] State Key Laboratory of Silicon Materials, Cyrus Tang Center for Sensor Materials and Applications, School of Material Science and Engineering, Zhejiang University, Hangzhou 310027, China.

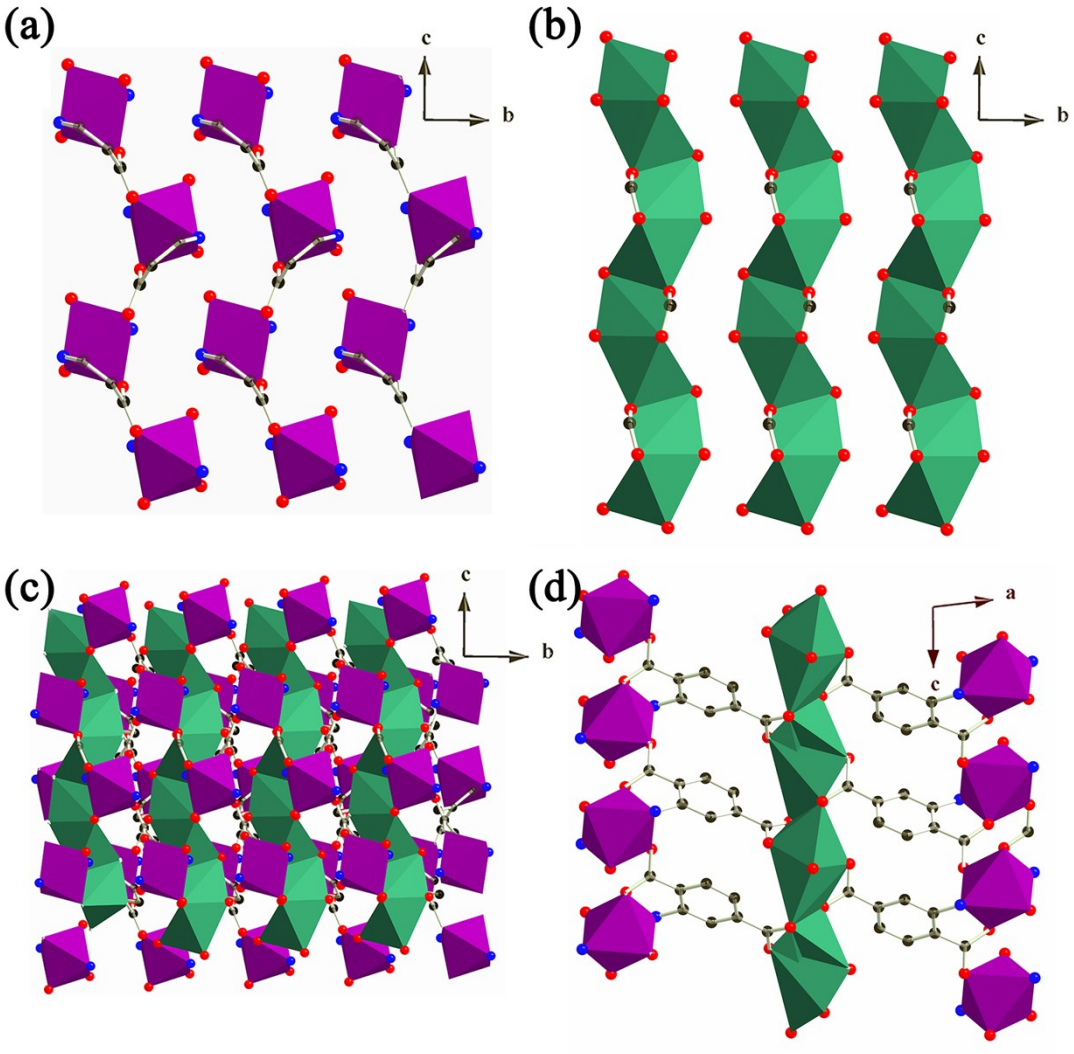

Figure S1. Crystal structure of ZJU-66.

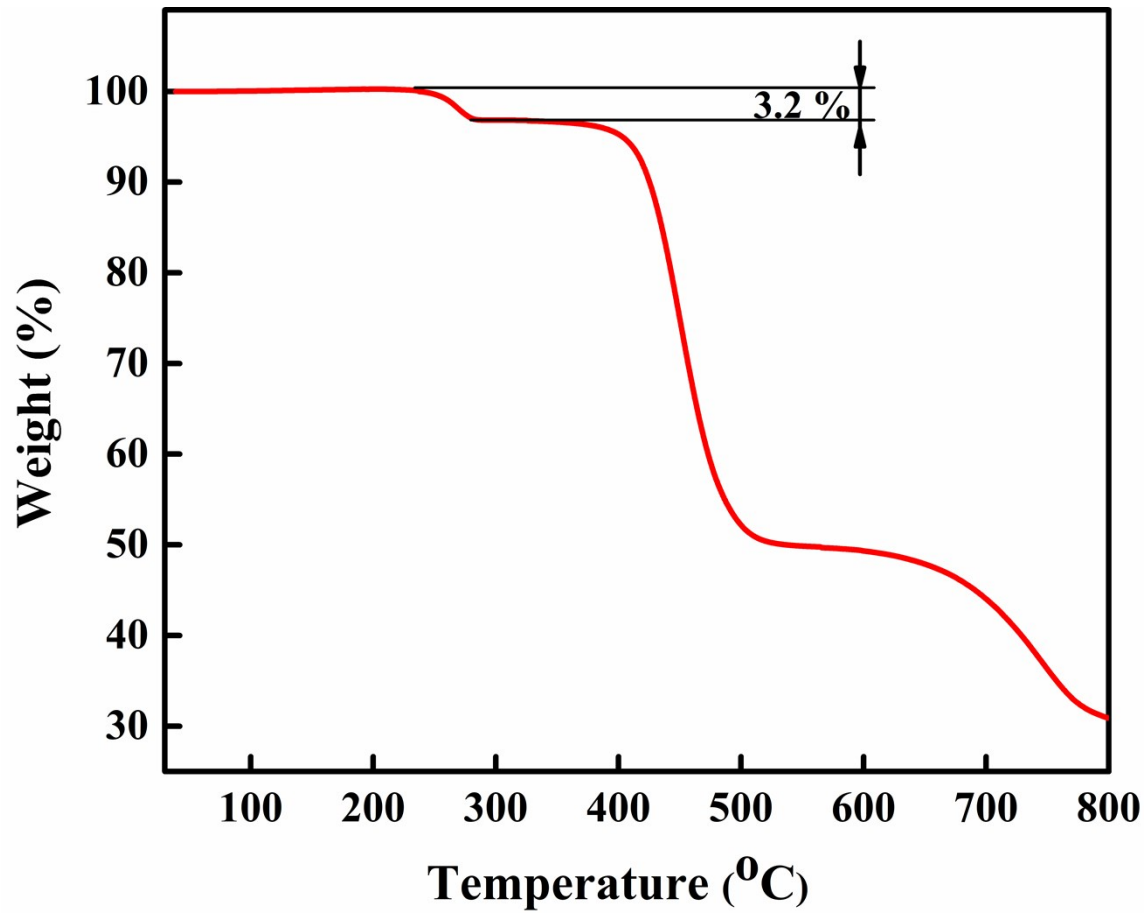

Figure S2. Thermal gravimetric analysis curves of ZJU-66

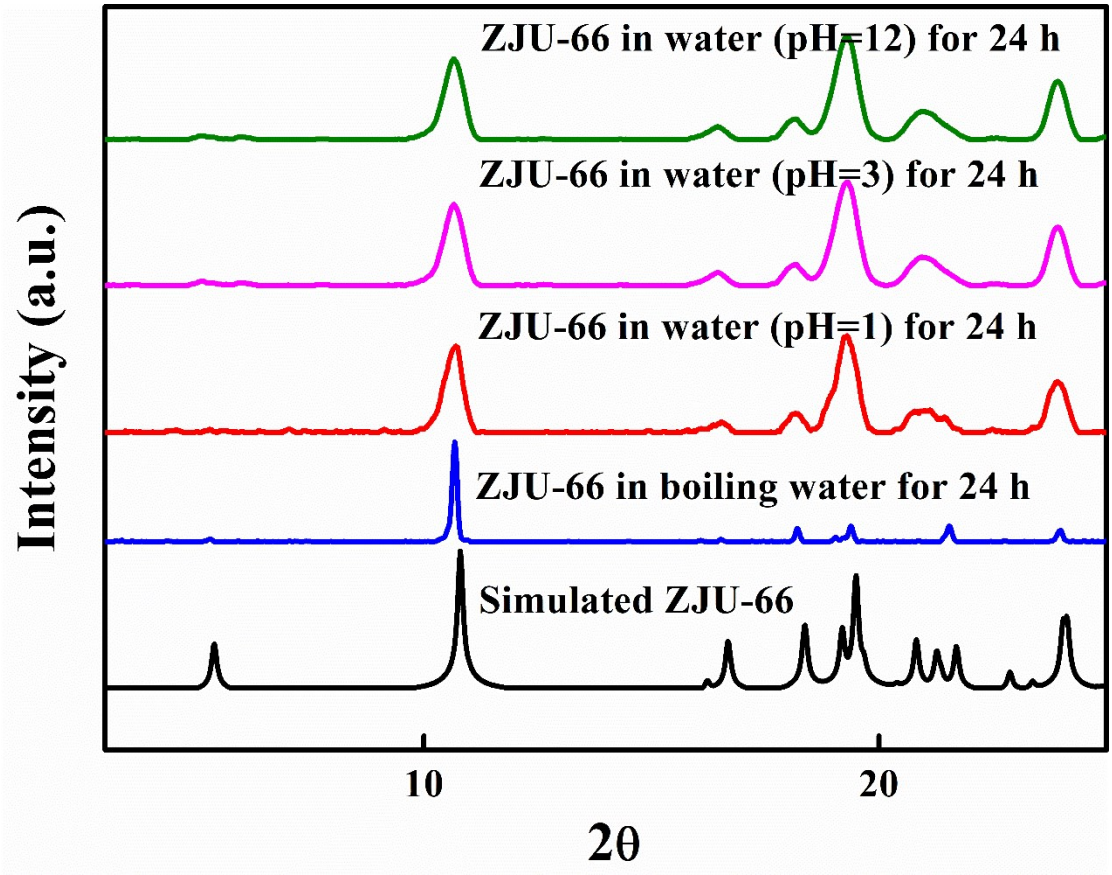

Figure S3. The XRD pattern of ZJU-66 after immersing in boiling water, acid solutions and basic solution for 24 h.

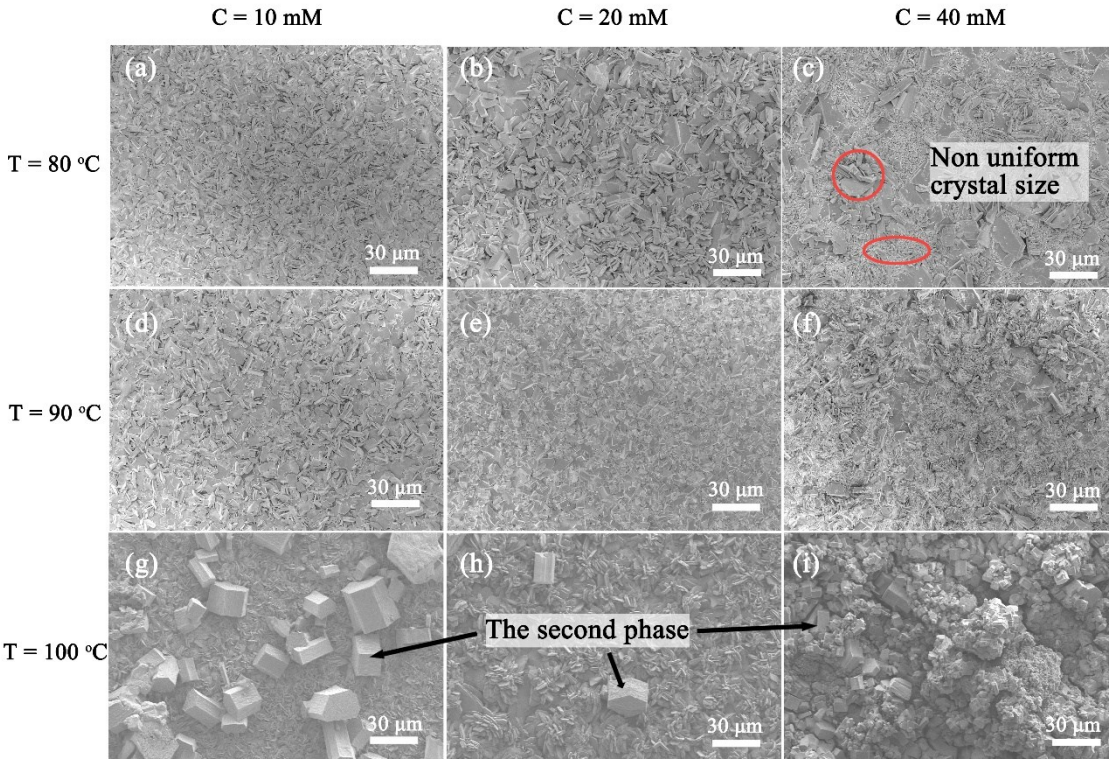

Figure S4. SEM images of ZJU-66 film supported on Zn metal plates prepared in the solvothermal solution with different concentrations of BDC-NH_2 and different temperature.

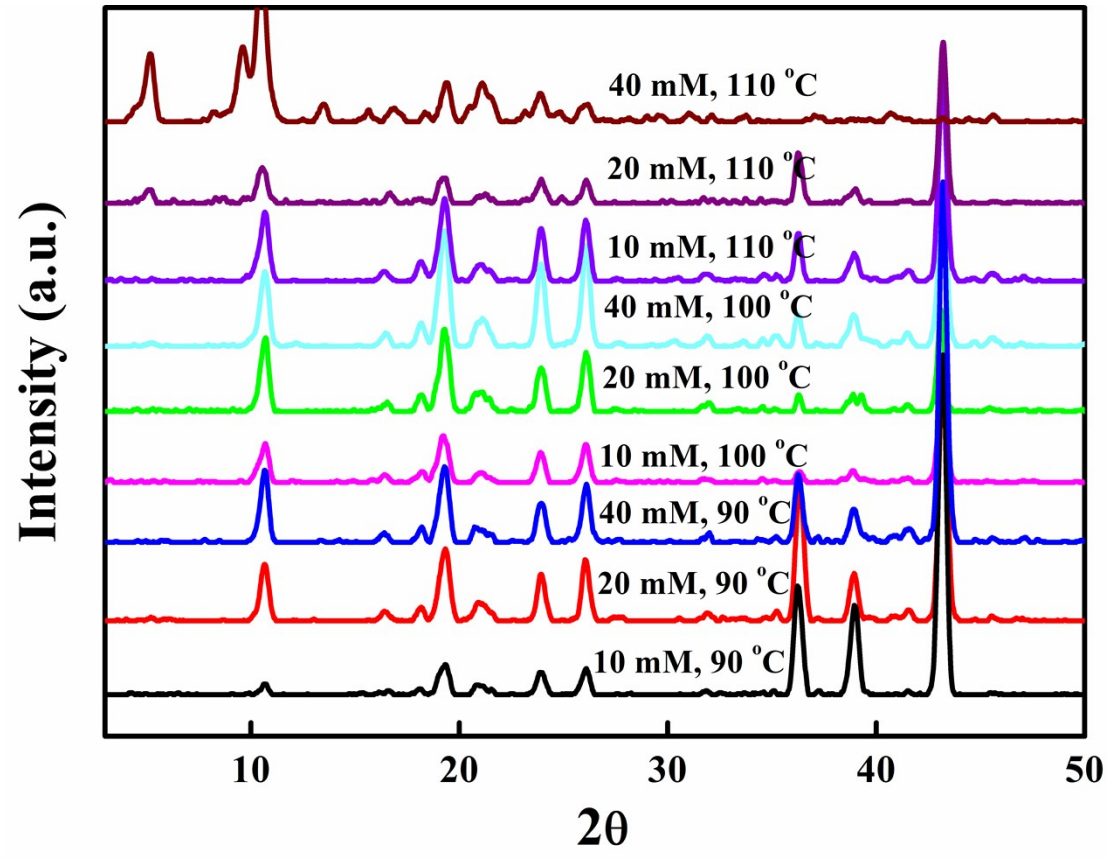

Figure S5. XRD patterns of as-synthesized ZJU-66 films at different ligand concentrations and temperature.

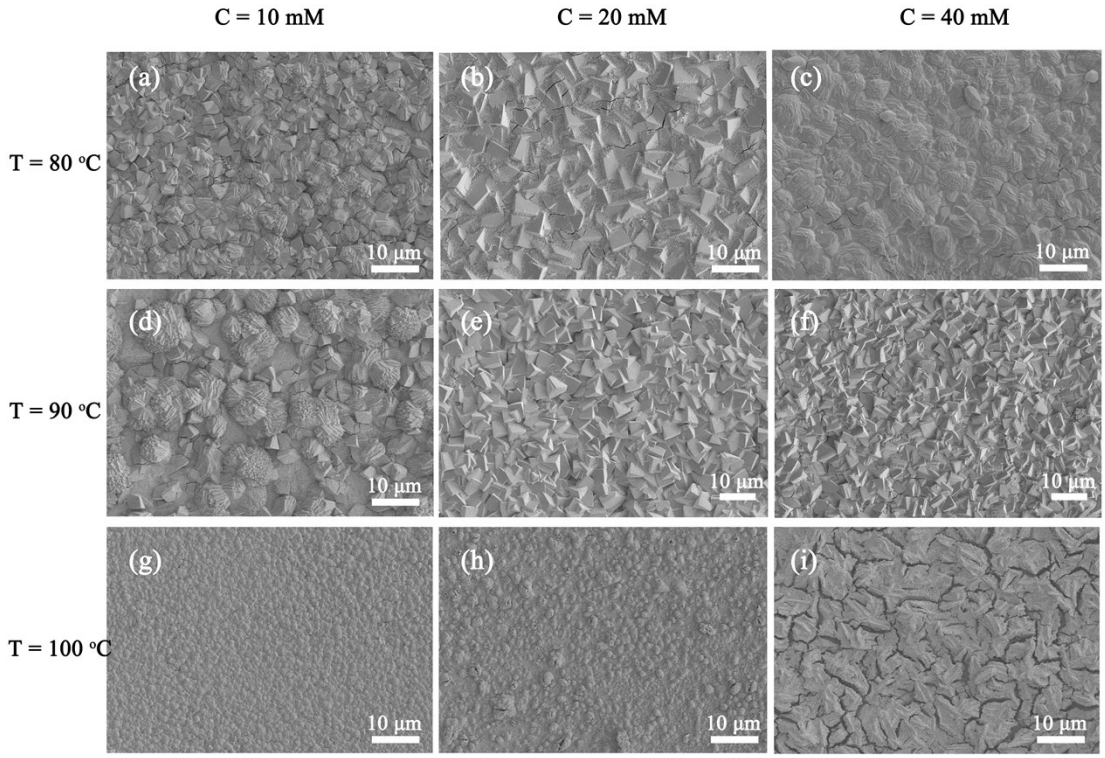

Figure S6. SEM images of MOF-5-$(OH)_2$ films supported on Zn metal plates prepared in the solvothermal solution with different concentrations of BDC-$(OH)_2$ and different temperature.

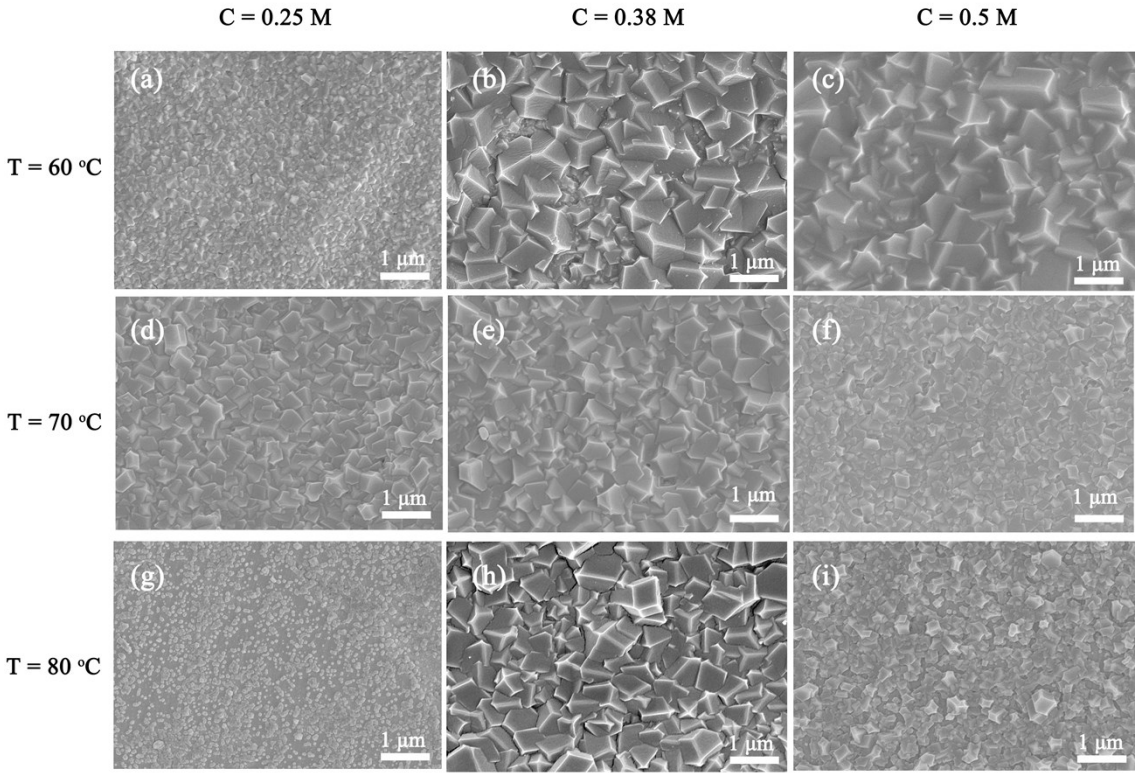

Figure S7. SEM images of ZIF-8 films supported on Zn metal plates prepared in the solvothermal solution with different concentrations of 2-MIM and different temperature.

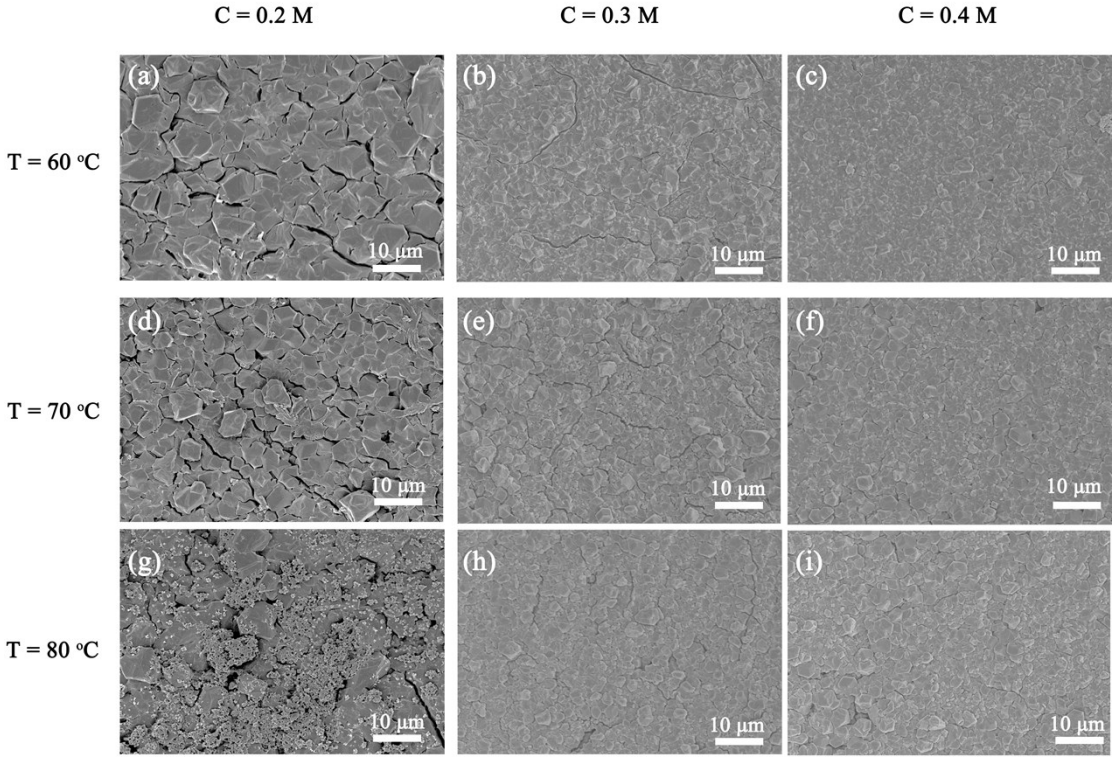

Figure S8. SEM images of ZIF-65 films supported on Zn metal plates prepared in the solvothermal solution with different concentrations of 2-NIM and different temperature.

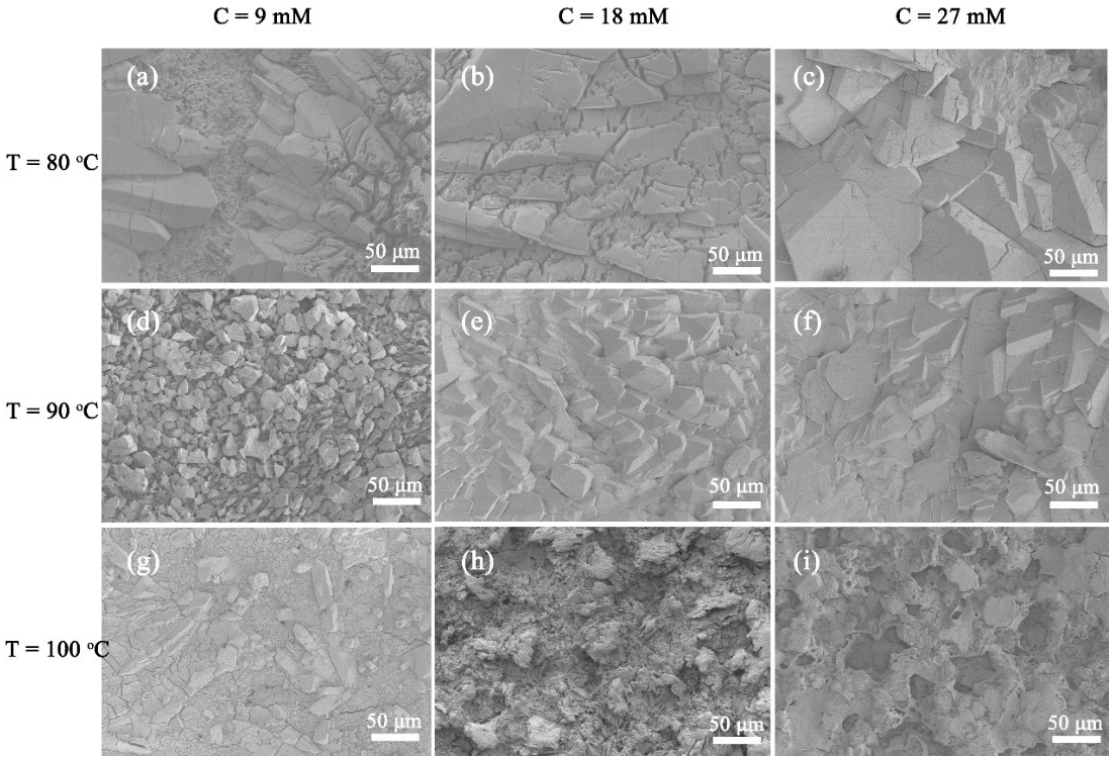

Figure S9. SEM images of Zn-BDC-COOH films supported on Zn metal plates prepared in the solvothermal solution with different concentrations of BDC-COOH and different temperature.

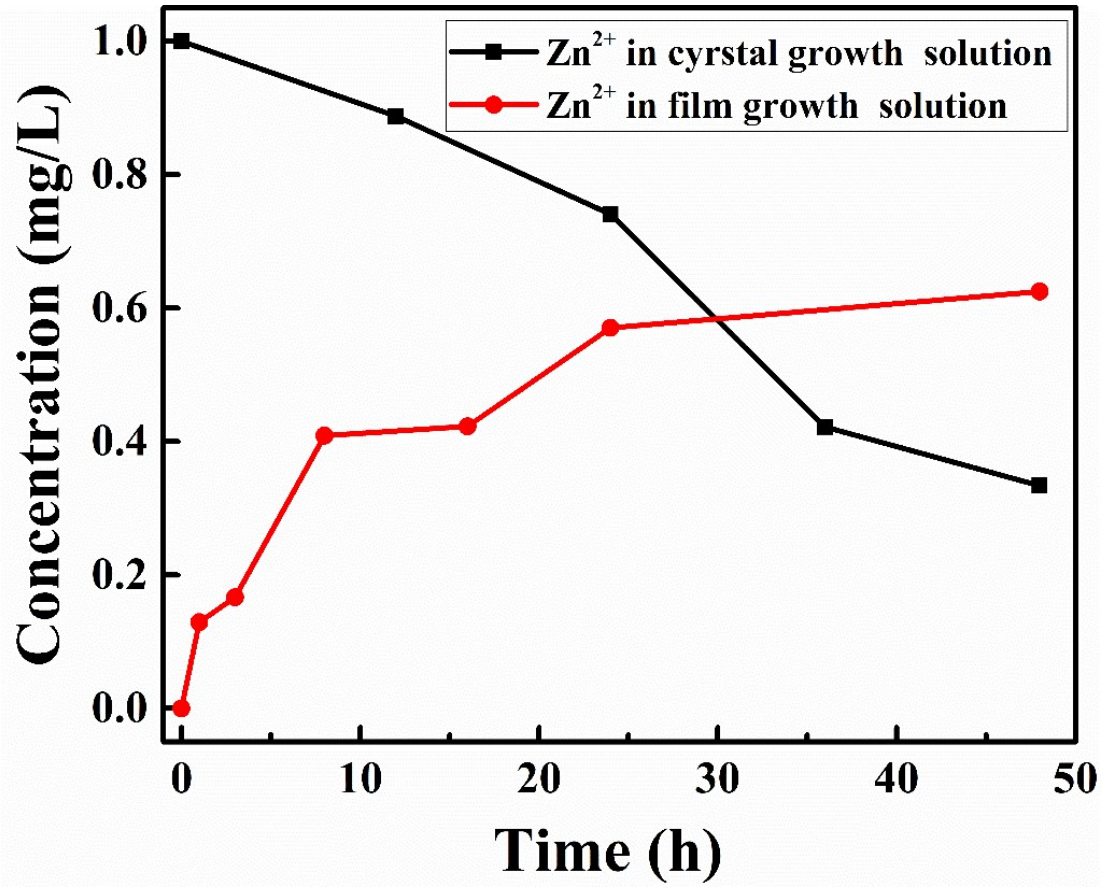

Figure S10. Zn^{2+} ions concentrations in Zn-BDC-COOH film growth solution and Zn-BDC-COOH crystal growth solution.

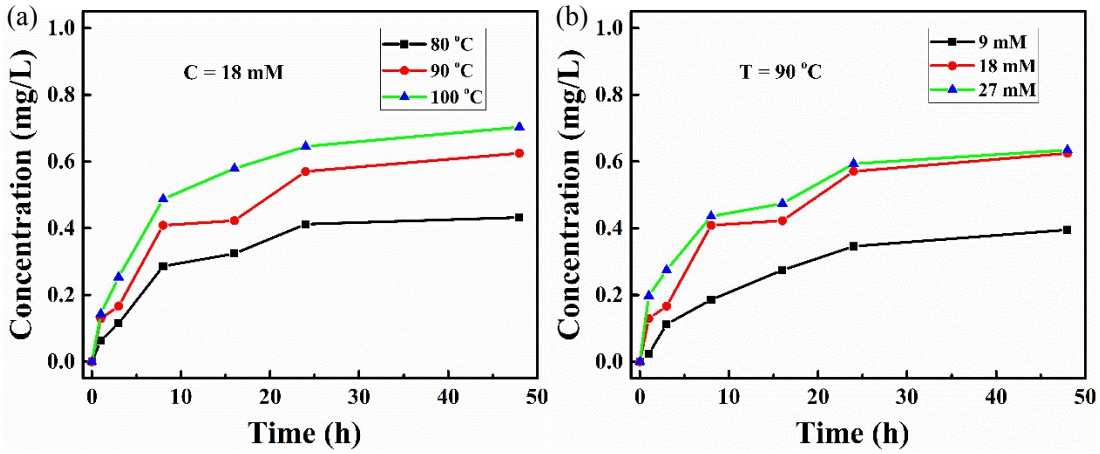

Figure S11. Zn^{2+} ions concentrations in Zn-BDC-COOH film growth solution with different (a) temperature and (b) ligand concentrations.

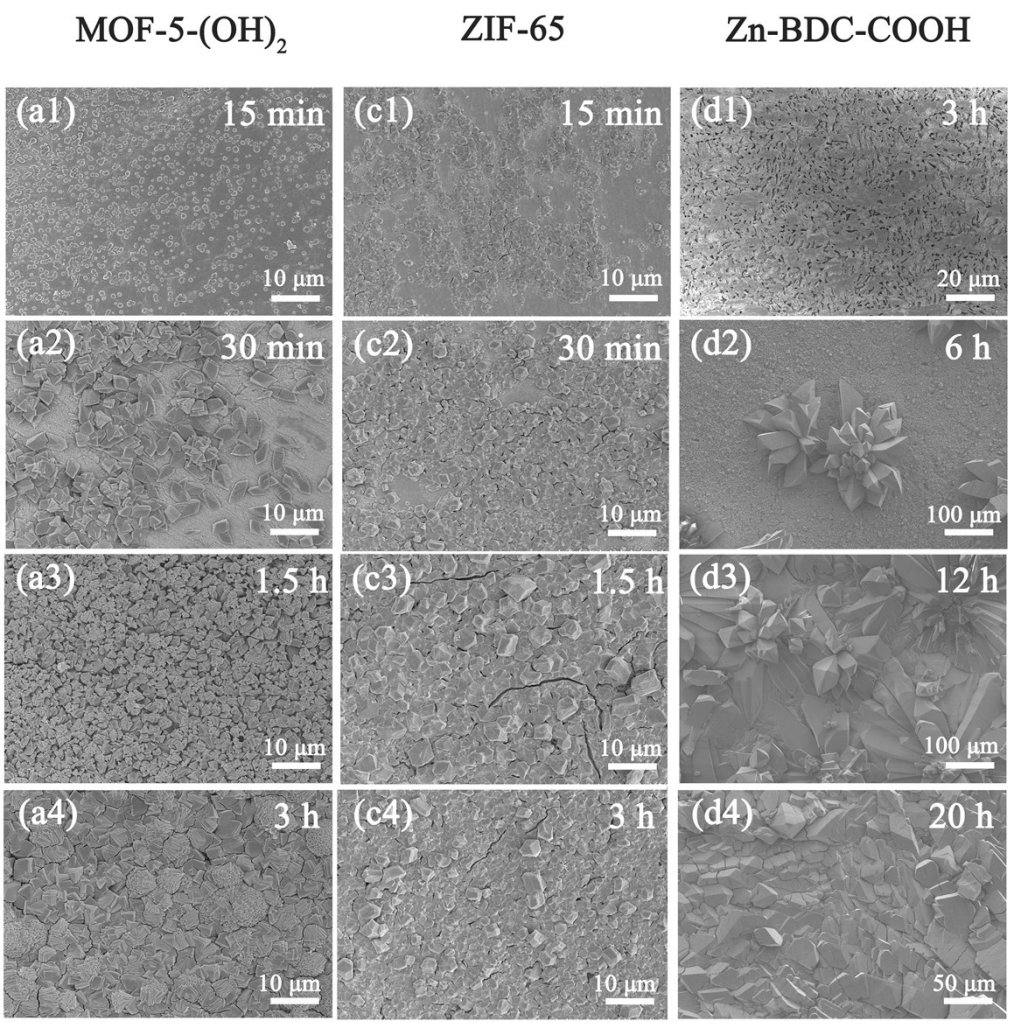

Figure S12. SEM images of MOF-5-$(OH)_2$, ZIF-65 and Zn-BDC-COOH films supported on Zn metal plates prepared in the organic linker solutions after different growth times.

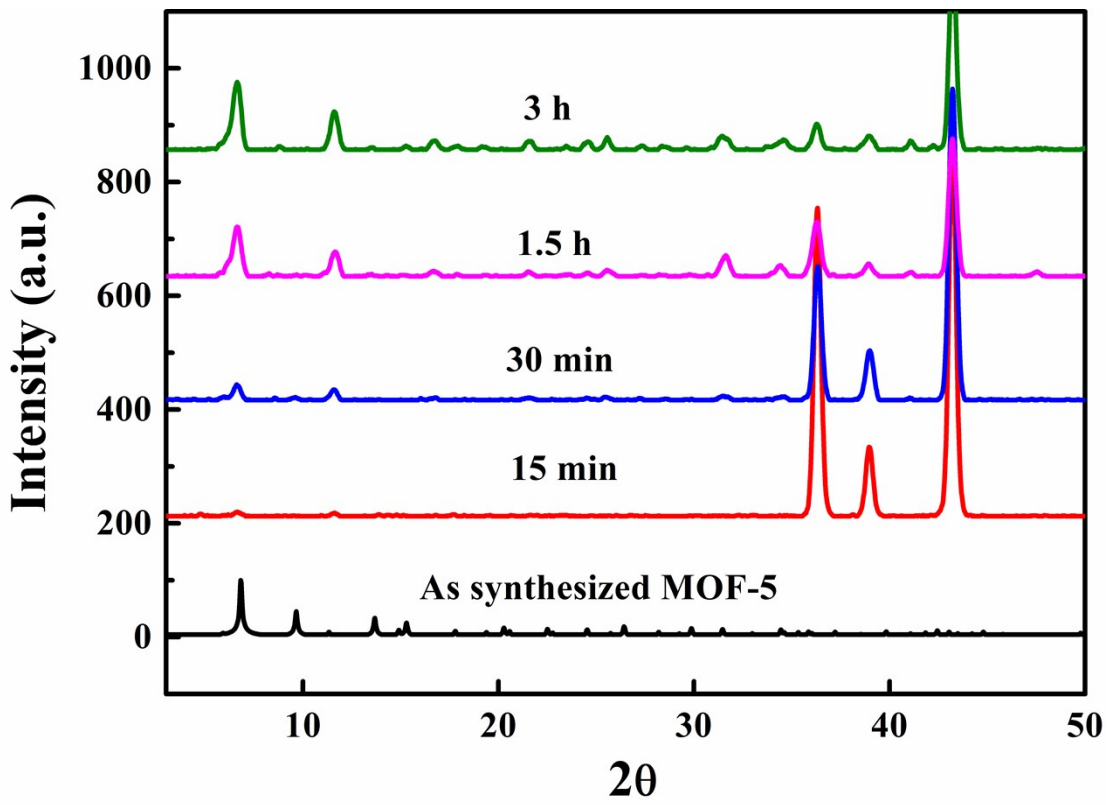

Figure S13. The XRD patterns of MOF-5-$(OH)_2$ films on zinc metal plates at different growth times.

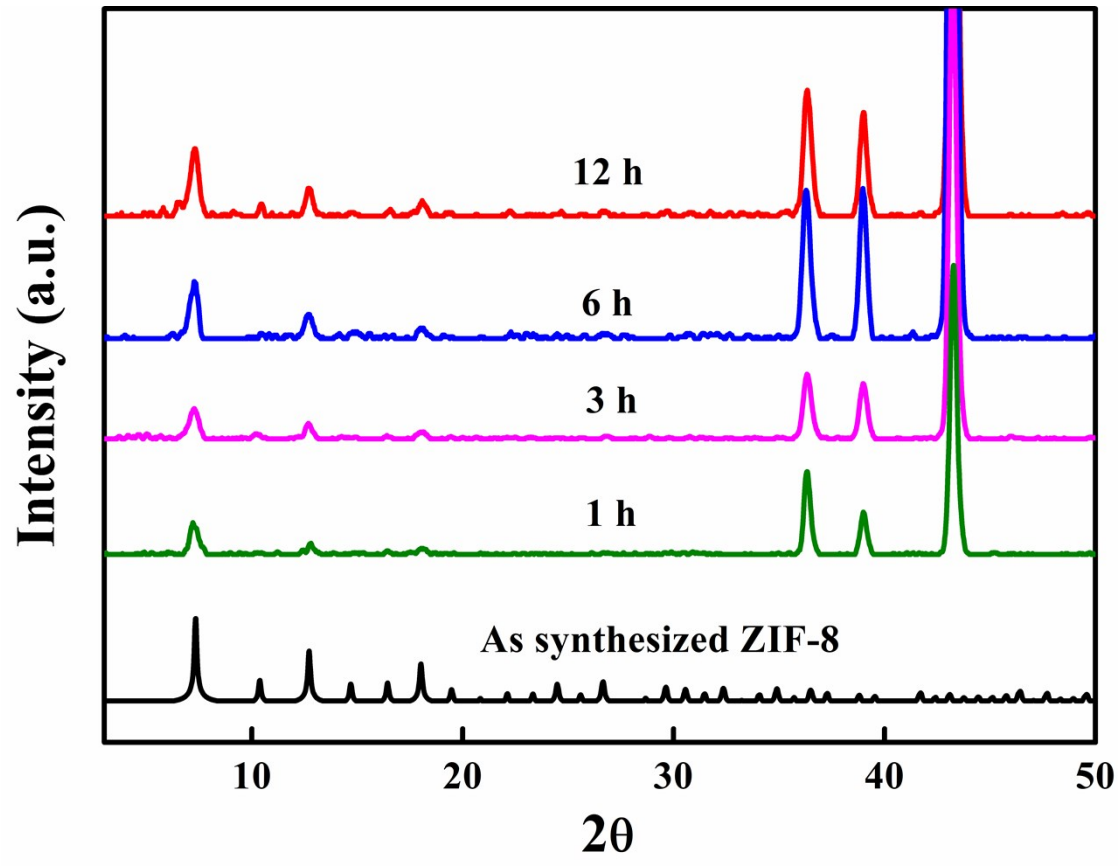

Figure S14. The XRD patterns of ZIF-8 films on zinc metal plates at different growth times.

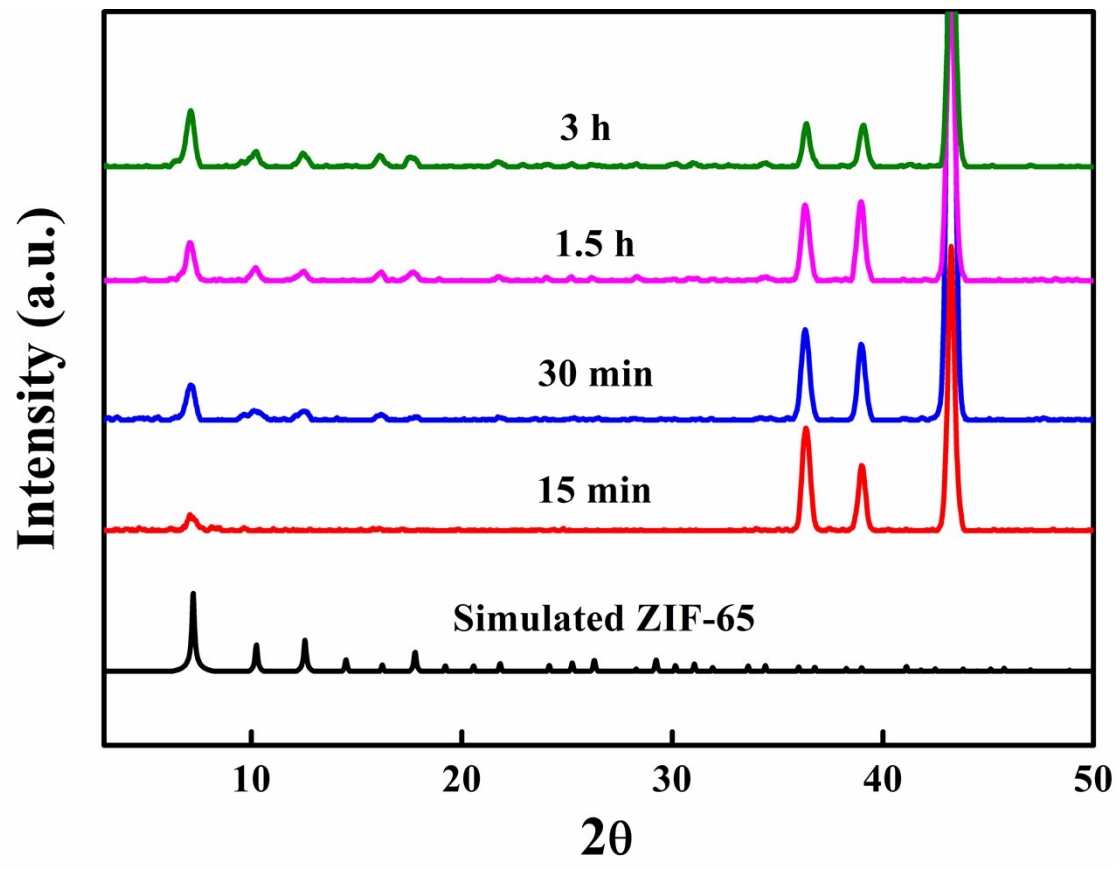

Figure S15. The XRD patterns of ZIF-65 films on zinc metal plates at different growth times.

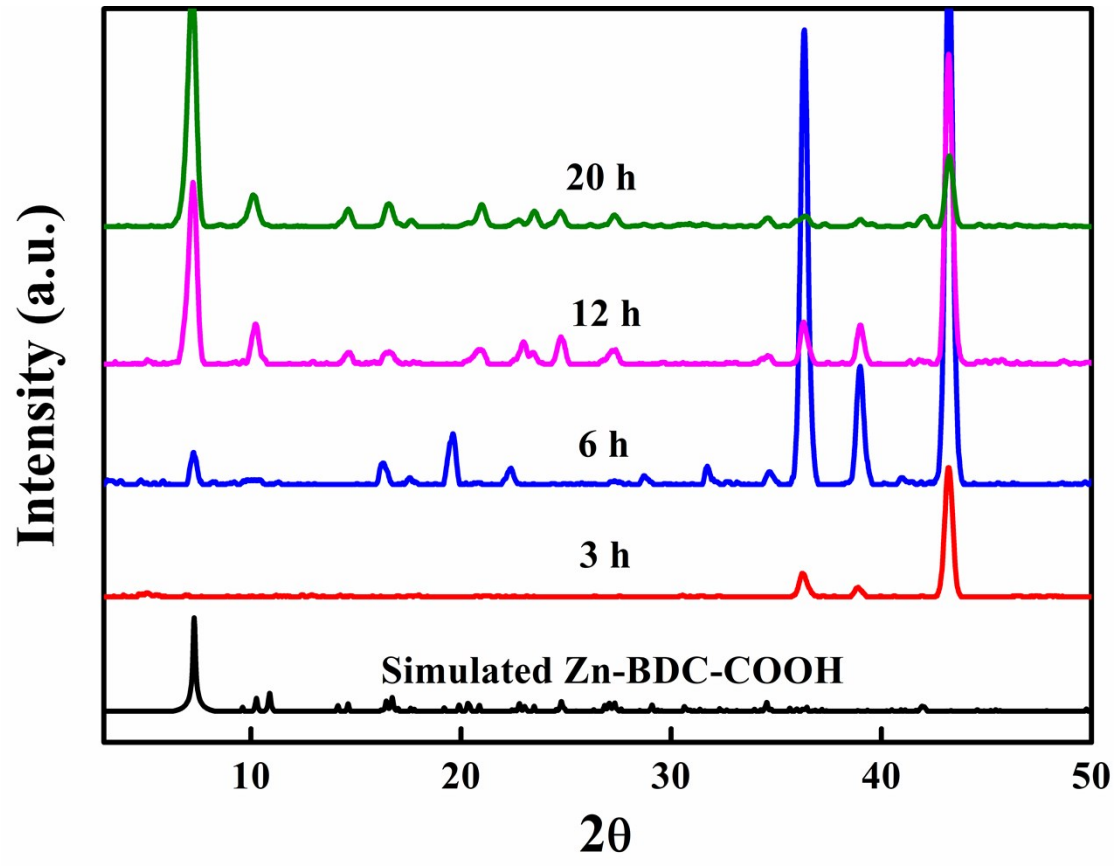

Figure S16. The XRD patterns of Zn-BDC-COOH films on zinc metal plates at different growth times.

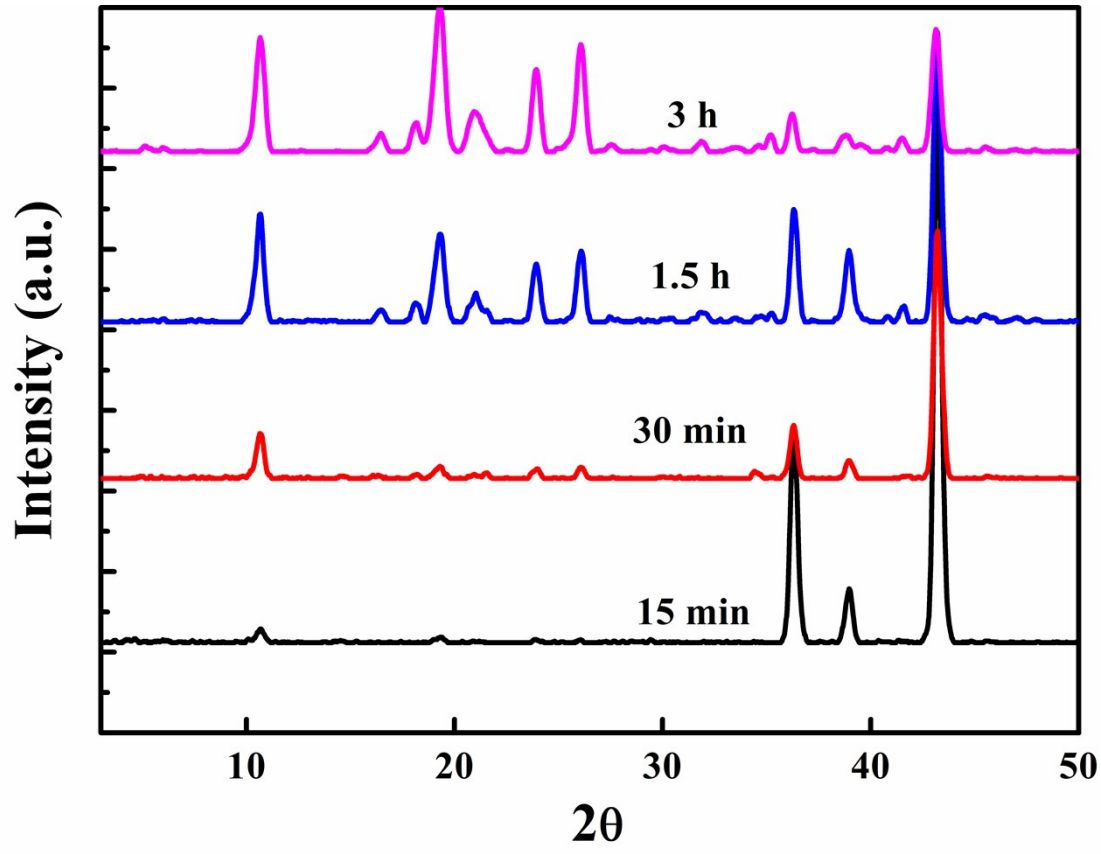

Figure S17. The XRD patterns of ZJU-66 films on zinc metal plates at different growth times.

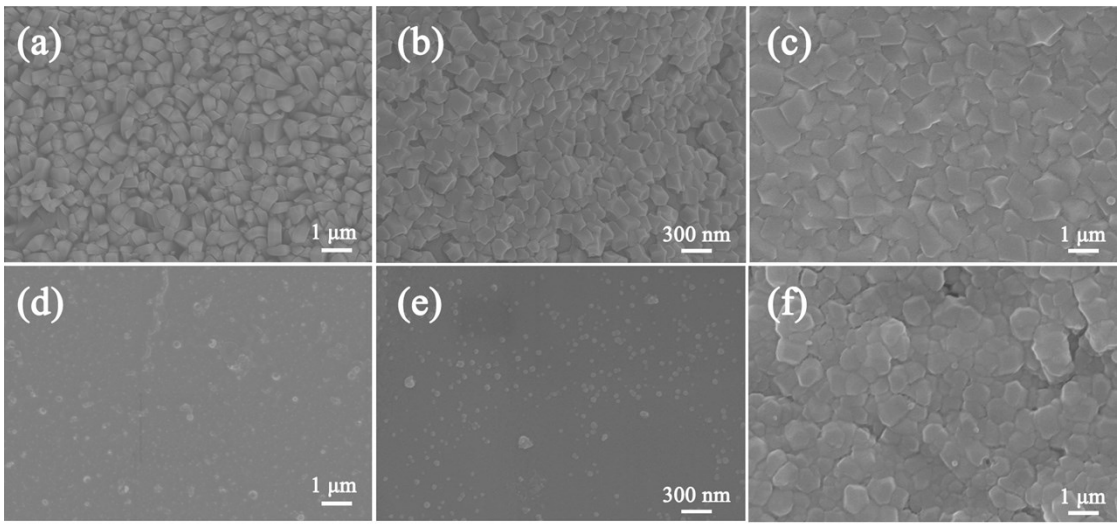

Figure S18. SEM images of ZIF-8 films synthesized on modified glass slides (a), silicon substrates (b) and metal plates (c); SEM images of ZIF-8 films on modified glass slides (d), silicon substrates (e) and metal plates (f) after corrosion treatments (put in NO_2 gas overnight and then sonicated for 30 minutes).

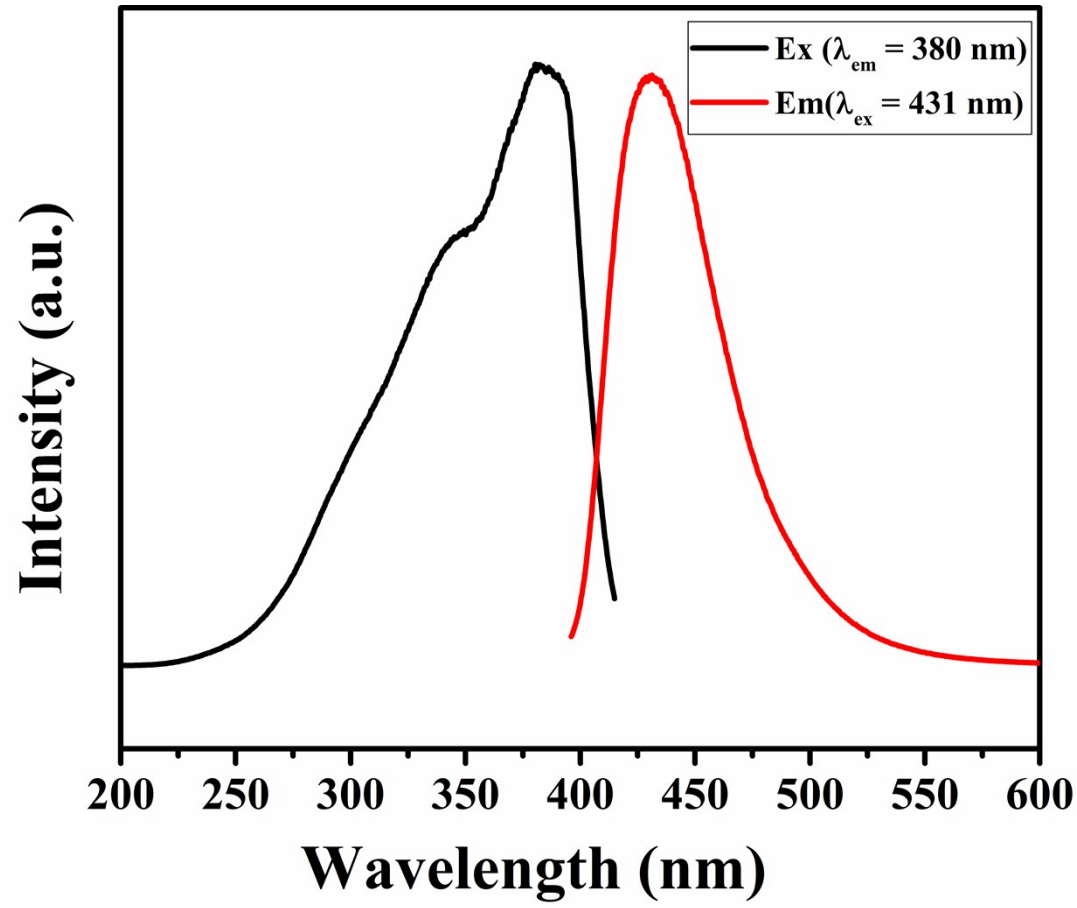

Figure S19. Fluorescence excitation and emission spectra of ZJU-66 film.

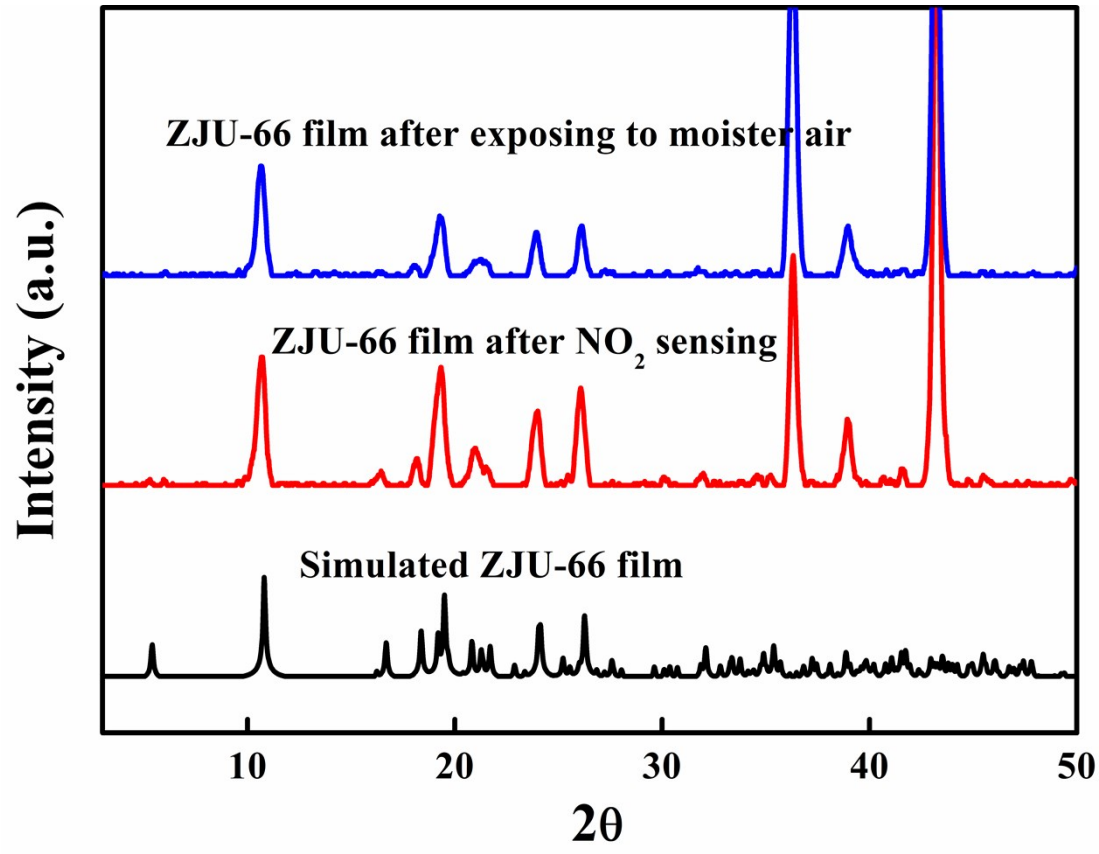

Figure S20. The XRD pattern of ZJU-66 films after NO_2 sensing and exposing to moister air.

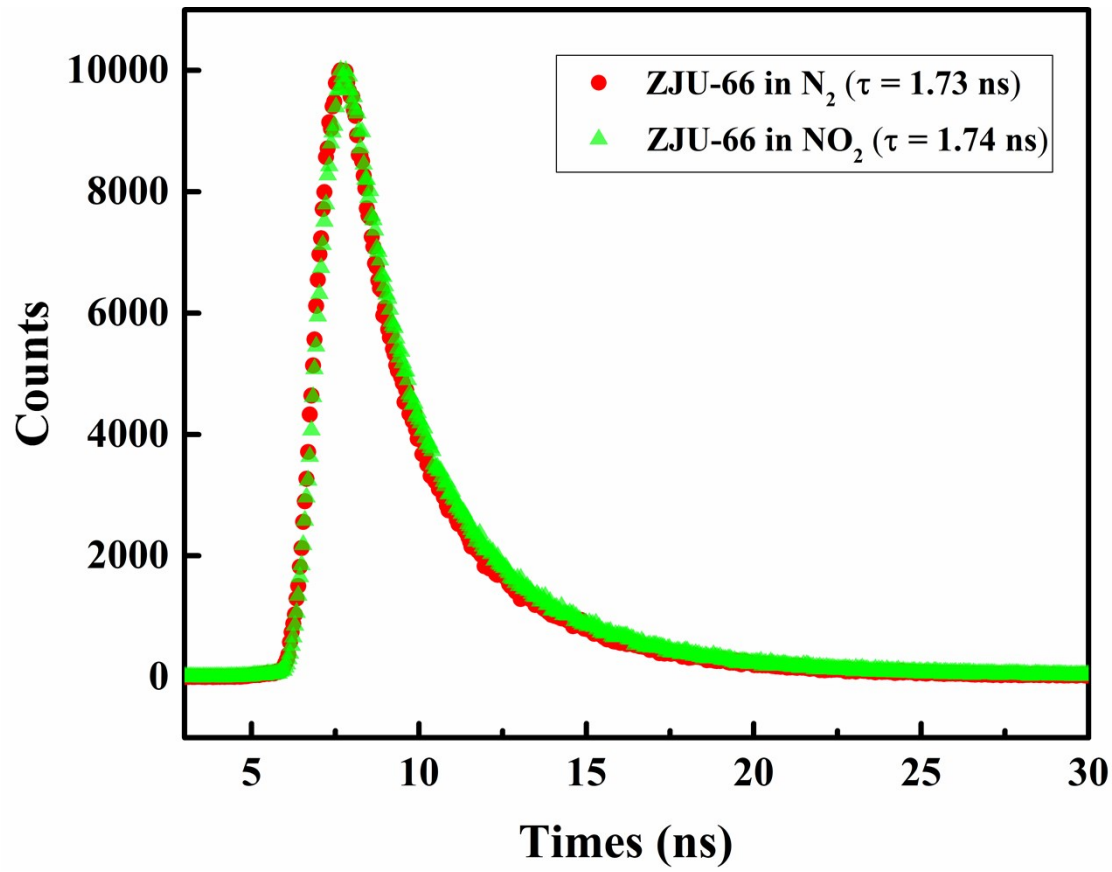

Figure S21. Time-resolved fluorescence decay curve of ZJU-66 film in N_2 and NO_2 atmosphere.

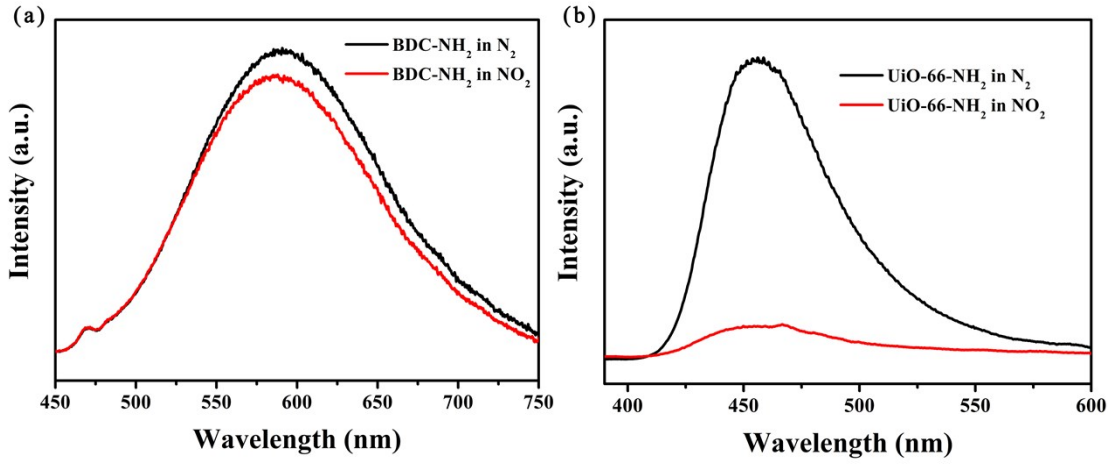

Figure S22. The fluorescence emissions of free ligand (a) and UiO-66-NH_2 (b) in absence and presence of NO_2 gas

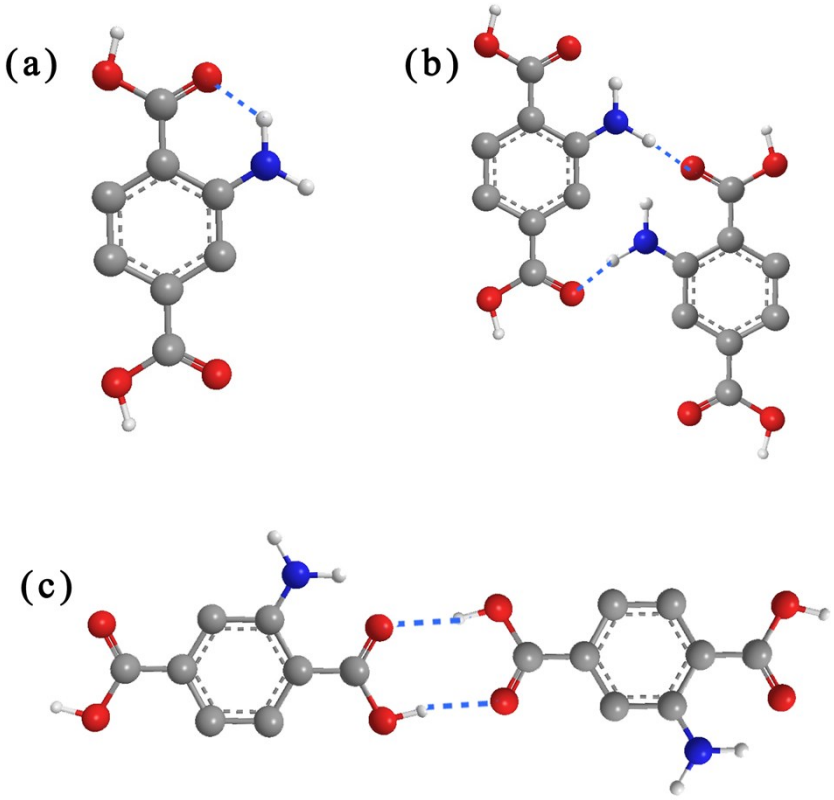

Figure S23. Three modes of intramolecular or intermolecular hydrogen bonding in ligands.

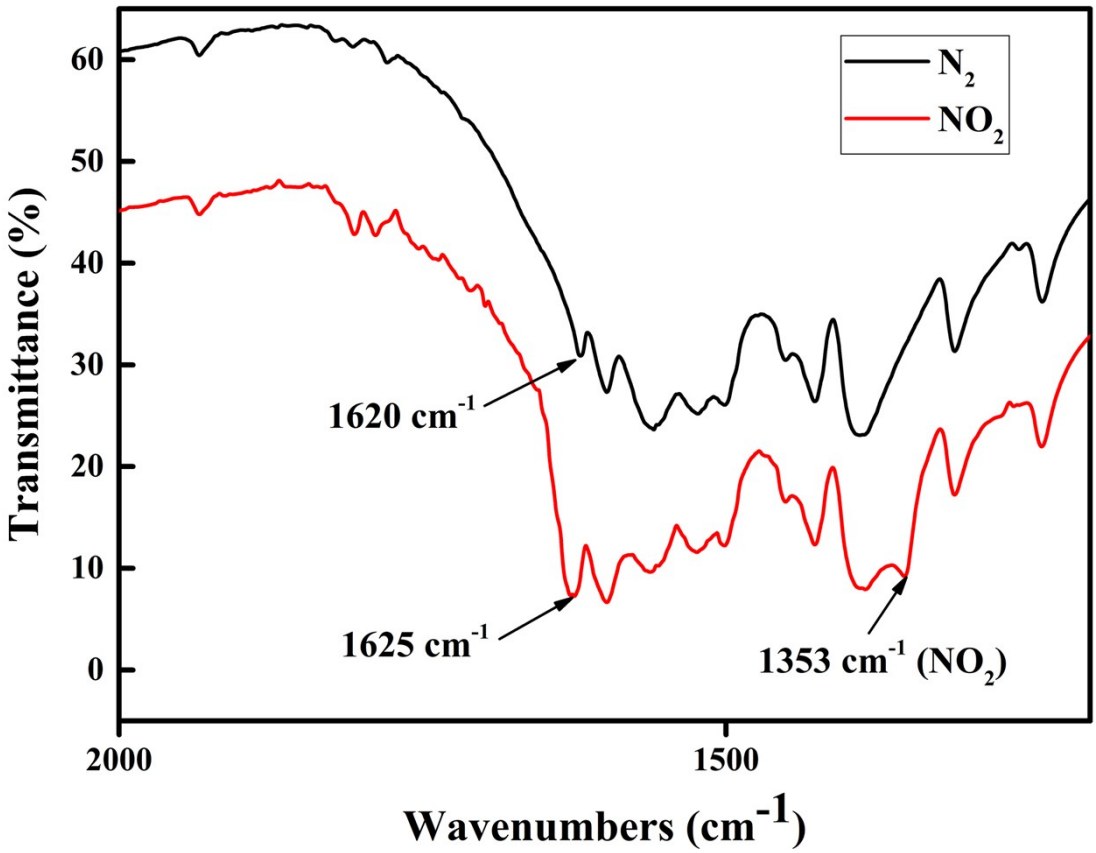

Figure S24. FTIR spectra of ZJU-66 film and the NO_2 exposed ZJU-66 film.

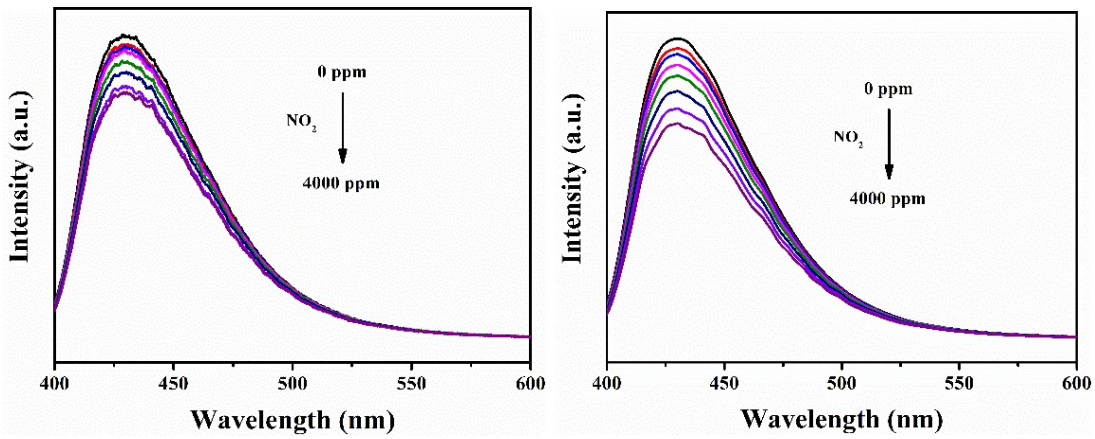

Figure S25. NO_2 sensing properties of ZJU-66 film grow for 30 minutes (left) and 3 h (right). ZJU-66 film that only grow for 30 minutes also exhibited sensing ability to NO_2, however, the quenching efficiency and the curve resolution is in comparable to ZJU-66 film that grow for 3 h.

Table S1. Crystallographic data and structure refinement results for ZJU-66.

Compound	**ZJU-66**
chemical formula	$C_{16}H_{12}N_2O_9Zn_2$
formula weight	507.02
crystal size (mm)	0.200×0.200×0.200
temperature (K)	173(2)
radiation	1.34139
crystal system	Monoclinic
space group	C c
a(Å)	32.9307(17)
b(Å)	5.3798(3)
c(Å)	9.1492(5)
α(°)	90
β(°)	96.282(2)
γ(°)	90
V(Å^3)	1611.14(15)
Z	4
ρ($_{calc}$) (g/cm^3)	2.090
F (000)	1016
absorp.coeff. (mm^{-1})	2.795
θ range (deg)	2.349 to 63.551
reflns collected	6987 (R_{int} = 0.0507)
indep. reflns	3468
Refns obs. [$I>2\sigma(I)$]	3343
data/restr/paras	3468 / 2 / 273
GOF	1.053
R_1/wR_2 [$I>2\sigma(I)$]	0.0403 / 0.1073
R_1/wR_2 (all data)	0.0420 / 0.1095
larg peak and hole(e/Å^3)	1.089 / -0.465

Table S2. The HOMO and LUMO energy level of the BDC-NH_2 monomer in N_2 and NO_2 atmosphere.

Atmosphere	HOMO	LUMO
N_2	-6.178 eV	-2.306 eV
NO_2	-7.235 eV	-3.081 eV